

A Critical Review of Human Jaw Biomechanical Modeling

Marco De Stefano *  and Alessandro Ruggiero 

Department of Industrial Engineering, University of Salerno, Via Giovanni Paolo II, nr. 132, 84084 Fisciano, Italy; ruggiero@unisa.it

* Correspondence: mardestefano@unisa.it

Abstract: The human jaw is a complex biomechanical system involving different anatomical components and an articulated muscular system devoted to its dynamical activation. The numerous actions exerted by the mandible, such as talking, eating or chewing, make its biomechanical comprehension absolutely indispensable. To date, even if research on this topic has achieved interesting outcomes using in vitro testing, thanks to the development of new apparatus and methods capable of performing more and more realistic experiments, theoretical modeling is still worthy of investigation. In light of this, nowadays, the Finite Element Method (FEM) approach constitutes certainly the most common tool adopted to investigate particular issues concerning stress–strain characterization of the human jaw. In addition, kinematics analyses, both direct and inverse, are also diffuse and reported in the literature. This manuscript aimed to propose a critical review of the most recurrent biomechanical models of the human mandible to give readers a comprehensive overview on the topic. In light of this, the numerical approaches, providing interesting outcomes, such as muscular activation profiles, condylar forces and stress–strain fields for the human oral cavity, are mainly differentiated between according to the joint degrees of freedom, the analytical descriptions of the muscular forces, the boundary conditions imposed, the kind of task and mandible anatomical structure modeling.

Keywords: biomechanics; biotribology; finite element analysis; human jaw; kinematics; multibody



Citation: De Stefano, M.; Ruggiero, A. A Critical Review of Human Jaw Biomechanical Modeling. *Appl. Sci.* **2024**, *14*, 3813. <https://doi.org/10.3390/app14093813>

Academic Editor: Arkady Voloshin

Received: 18 March 2024

Revised: 16 April 2024

Accepted: 26 April 2024

Published: 29 April 2024



Copyright: © 2024 by the authors. Licensee MDPI, Basel, Switzerland. This article is an open access article distributed under the terms and conditions of the Creative Commons Attribution (CC BY) license (<https://creativecommons.org/licenses/by/4.0/>).

1. Introduction

Biomechanics is a discipline involving the study and analysis of the movement of biological entities originating from external forces [1]. Hence, it consists of the application of mechanical laws to determined biological systems such as hips [2], knees [3], ankles [4] and so on. Biomechanics is a wide field including several subfields: biotribology [5–7]; computational biomechanics, in particular the Finite Element Method (FEM) [8–11]; nature bio-inspired mechanisms and so on. In light of this, the mandible is a clear example for which the relevance of investigations in this engineering area is paramount to the longevity of any kind of prosthesis, such as dental implants [12] or more articulated structures [13]. Indeed, the definition of the forces transmitted [14], the kinematics of the entire biosystem and calculation of the efforts diffused in the coupling may help clinicians and engineers to design and contribute to them designing sophisticated and customized structures for patients, taking into account also the clinical conditions [15] with the aim of the prosthesis's long-term survival. To achieve this, the process of osseointegration [16,17] is almost indispensable in terms of the correct and stable growth of the bone in proximity to the medical structure. In this sense, it is widely accepted that the bone remodels itself accordingly to the stress imposed. In fact, as confirmed by Wolff and Frost's studies, there is a direct relationship between the strain and the biological reaction [18]. Moreover, thanks to technological development, interesting scenarios can be analyzed, such as facial injuries caused by ballistic impacts [19] and mandible reconstructions using plates, as indicated by Bujtár et al. [20]. Indeed, one of the most critical issues is potential fracture of the mandible, which requires specific medical treatments [21]. In any case, the human jaw is basely a structure articulated with the left and right condyles, which plays a key role in

common daily activities, both static, such as biting, and dynamic, such as eating, swallowing and speaking. From a mechanical perspective, the temporomandibular joint (Figure 1) is characterized by three degrees of freedom [22], indicated by anterior–posterior and mediolateral translations, respectively, in the sagittal and transverse planes and rotation, again in the sagittal plane (Figure 2). In further detail, this rotation is referred to as disk–condyle coupling, whereas the disk–articular fossa translations correspond to the superior joint cavity because the former is not tightly attached to the latter. Nevertheless, in several simulations, it is modeled as a fixed constraint, blocking all possible translations and rotations [23–25].

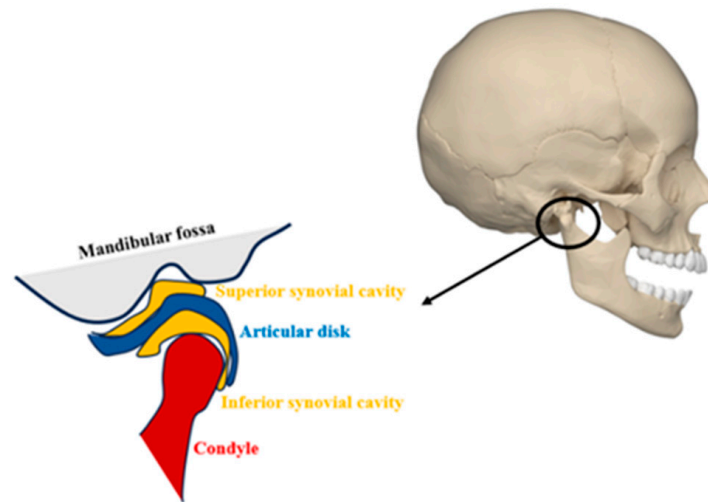


Figure 1. The temporomandibular joint anatomy.

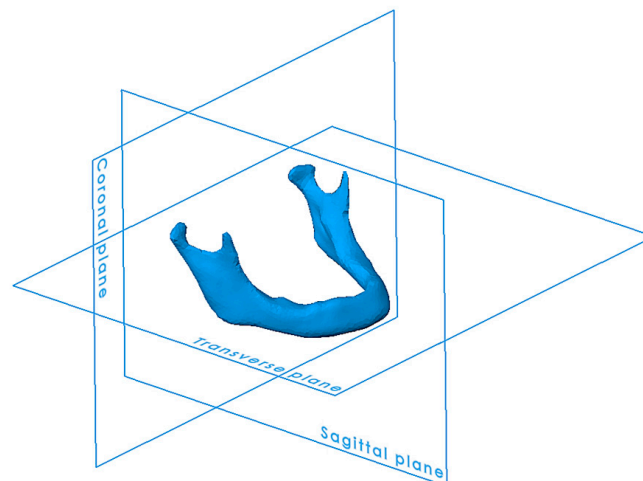


Figure 2. Sagittal, coronal and transverse planes of mandible CAD file.

It is coupled with diverse muscular activations, permitting five kinds of movements [26,27] (Figure 3):

- *Elevation*, corresponding to the closing of the mouth
- *Depression*, corresponding to the opening of the mouth
- *Protrusion*, corresponding to the protraction of the chin
- *Retraction*, corresponding to the retraction of the chin
- *Lateral motions* (side to side)

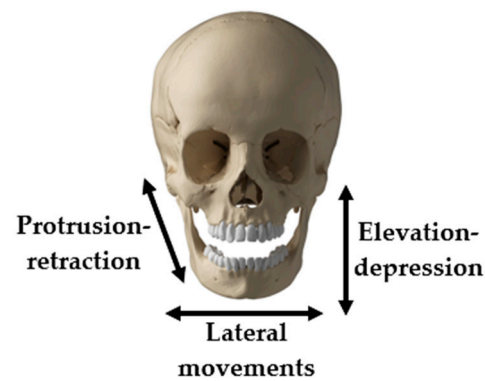


Figure 3. Human skull CAD files with mandible movements in their respective directions.

In particular, the muscles responsible for oral cavity movements are essentially four [28,29]: the masseter, divided into deep and superficial parts; the temporalis, divided into anterior, middle and posterior; the medial pterygoid and the lateral pterygoid (Figure 4), although others are also influential, such as the digastric muscle [30] or the suprahyoid muscles [31]. During a specific action, the muscles can activate and combine in several ways [32], which is the reason why they are not commonly understood as unique and independent units. However, the larger ones are supposed to produce more isometric forces than the smaller muscles [33], as confirmed by electromyography (EMG) [34,35]. Moreover, there is a clear asymmetry between the muscular forces acting on the working and balancing sides, which can be expressed analytically using scaling factors. The product of these coefficients and of the muscular loads provides the force magnitude, explicated in the three directions x , y , z using unit vectors successively integrated into the FEM's boundary conditions, as undertaken by Saini et al. [36]. This approach is appropriate on the condition that the muscle tissues studied are anchored to bone so that the muscle forces can be generated [37]. Finally, the latter can be calculated experimentally or numerically, as calculated by the duo Koriath and Hannam during mastication tasks [38,39].

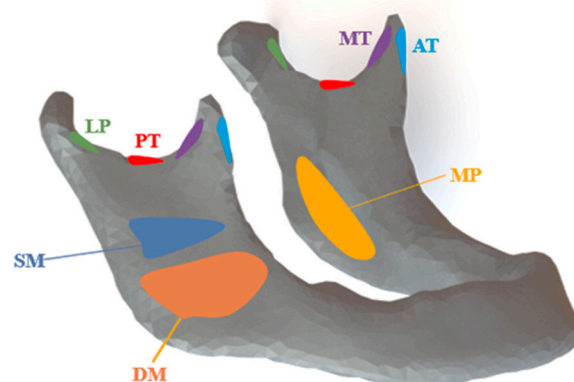


Figure 4. Human jaw muscle attachment: lateral inferior pterygoid (LP) in green, posterior temporalis (PT) in red, middle temporal (MT) in violet, anterior temporalis (AT) in pale blue, medial pterygoid (MP) in ochre, superficial masseter (SM) in blue and deep masseter (DM) in orange.

The current state of art provides both experimental [40], through the use of strain gauges, photoelasticity or innovative approaches like image correlation, as proposed by Yachouh et al. [41], and numerical tests [42]. The clear advantages offered by the latter in terms of their non-invasive techniques, the simplicity ensured by high-performance software and especially their good agreement with experiments [43] make them a valid and popular alternative, as confirmed by Knoell's study [44]. The flow process involves a computer tomography (CT) scan image of the jaw, solid conversion using 3D CAD tools

and mesh construction [45]. Nevertheless, numerical models are usually based on exemplifying imposed hypotheses [46] such as the idea that the bone properties are intrinsically anisotropic and not homogenous [47]. Consequently, their comparison with in vivo trials is necessary to validate their results. In this regard, Craig et al. [48] evaluated experimentally the biomechanical behavior of the mandible when the chin was loaded. The forces and displacements were thus extrapolated, acting as the basis for computational models. Alvarez-Arena et al. [49] investigated, via a computational approach, the biomechanics of the jaw during three movements, middle and maximum opening and protrusion, at different bone mineral densities, finding out that the latter determined the highest deformation, mostly corresponding to the mandibular angle. Meira et al. [50] proposed an experimental setup for calculating the mandible's stiffness without any constraints. In this regard, a point of distinction is the physical nature of the jaw, which can be extrapolated from human cadavers or be purely animal in origin, as with pigs or sheep. An alternative is realization using additive manufacturing, as carried out by De Santis et al. [51] by adopting a poly(methyl methacrylate) core and glass fiber reinforcement.

Overall, to our knowledge, the review manuscripts regarding mandible biomechanics have essentially focused on the methods of reconstruction [52], edentulous conditions [53], the stress patterns during mastication [54], or reference to peculiar zones, such as the temporomandibular joint (TMJ) [55]. Wong et al. [56] proposed an overview of all the biochemical models, both physical and computational. On the contrary, our aim is to analyze and discuss from a more computational perspective the biomechanics of this biological apparatus, accenting the roles of the muscular forces and the temporomandibular joint and their interaction.

2. Materials and Methods

The mathematic modeling of mandible biomechanics is certainly an ongoing and fascinating field of bioengineering. Indeed, it has captured the attention and the curiosity of clinicians and engineers since 1970s [57] when the first experiments were performed. Nowadays, the use of any kind of model is only investigative, with no applications to diagnostic protocols [58], via cause–effect scenarios: the aim is to rapidly obtain the outputs desired by varying the boundary conditions. In light of this, the evident complexity of the human jaw should be taken into account in terms of its geometry, mechanical properties, muscle activations and so on. Moreover, each patient has a specific conformation from a morphological point of view, which can be described using only seven morphometric measurements, as stated by Vallabh et al. [59]. Since the jaw shape is extremely intricate, ascertaining its geometry is achieved using a CT scan, which is successively refined or modified [60]. Secondly, the entire coupling, composed of muscles, ligaments and bone, must be described according to its mechanical and physical properties. For instance, the anisotropic property of bone has a great influence on the stress–strain regime [61] but causes greater computation efforts. Hence, numerical models are based on the trade-off between realistic behavior and the equation resolution time.

Muscle, joint and tendon modeling, instead, is essentially based on the multibody theory, in which the joints are characterized using Equation (1):

$$\{\Phi(q, t)\} = 0 \quad (1)$$

This indicates the set of algebraical constraints on the generalized coordinate vector q at the interval of time t . These can be divided into time-independent constraints like anatomical ones or constraints as a function of time, such as the muscle length during the performed action. The choice of the coordinates q depends on the specific investigation, but they usually refer to the condyle process, muscle insertions and biting force origins. Furthermore, the latter are referred to according to the x , y and z axes, outlining, respectively, the anterior/posterior, lateral and inferior–superior directions [62].

By amending Equation (1) twice with respect to the time, we obtain:

$$[\Phi_q](\ddot{q}) = [\gamma] \tag{2}$$

where γ refers to the constraint's quadratic velocity tensor, equal to:

$$\gamma = -\left(\Phi_{q\dot{q}}\right)_q \dot{q} - 2\Phi_{q,t}\dot{q} - \Phi_{t,t} \tag{3}$$

in which Φ_q is the constraint's Jacobian matrix; \dot{q} and \ddot{q} are the first and second derivatives of coordinate q , corresponding, respectively, to the velocity and acceleration vector of the generalized coordinates; $\Phi_{q,t}$ is the constraint's Jacobian matrix's first partial time derivative and $\Phi_{t,t}$ the constraint vector's first partial time derivative. These relationships are thus coupled with the motion laws (Equation (4)), providing an algebraic-differential system of equations (DAE):

$$[M](\ddot{q}) = (F^i) + (F^e) = F \tag{4}$$

$$\begin{bmatrix} M & \Phi_q^T \\ \Phi_q & 0 \end{bmatrix} \begin{Bmatrix} \ddot{q} \\ \lambda \end{Bmatrix} = \begin{Bmatrix} F \\ \gamma \end{Bmatrix} \tag{5}$$

where $[M]$ is the mass matrix, and F^i and F^e are vectors of all the internal (muscles, ligaments) and external forces (gravity, ground reaction). Finally, λ represents the Lagrange multiplier vector, indicating the joint reaction forces. The mathematical system reported in (5) can be approached using both forward and inverse analysis. The first technique is adopted when the forces are determined using electromyography [63], and the position vector must be evaluated: \ddot{q} and λ are therefore solved in Equation (5) and successively integrated to obtain the position and velocity vector. This procedure is repeated for all the time steps imposed by the analysis. On the other hand, the inverse dynamics uses jaw movements extrapolated experimentally via optical techniques [64] to calculate the forces and time steps applied. Both the methodologies involve sets of equations whose analytical solution is unique only if the number of equations is exactly the same as that of the unknown variables. When the equality is not respected, an optimization problem (Equation (6)) should be considered, characterized by an objective or cost function that may be minimized or maximized according to the set of equality and inequality constraints.

$$\begin{Bmatrix} \min f(x) \\ Ax = b \\ A'x' \leq b' \end{Bmatrix} \tag{6}$$

The function $f(x)$ can measure the difference between numerical and experimental results, individual muscular forces or stress [65]. The most common model for describing muscular activities at the microscopic level is certainly Hill's [66] and its variants [67], for example, adopting a pennation angle between the tendon traction line and muscular fibers [68] or the viscosity of the muscle [69]. According to his theory [70], a muscular unity can be built as shown in Figure 5. The contractile element (CE) is the active component [71] determined by the cross-bridges formed between the two proteins of the sarcomere unit, myosin and actin [72]. Two non-linear springs are also introduced: the series element (SE) directly connected to the CE, representing the tendon and the elasticity of the myofilament, and the parallel element (PE), indicating the elasticity of connective tissues such as the epimysium, perimysium and endomysium.

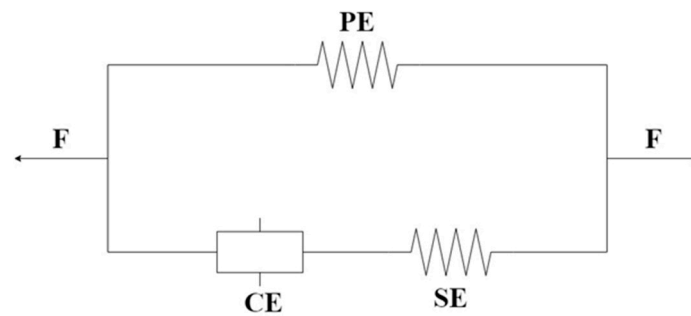


Figure 5. Muscular units of Hill's model. PE is the parallel element, SE the series element, CE the contractile element and F the muscle force.

For this configuration, the following relationships both for the forces (Equation (7)) and length L (Equation (8)) must be satisfied:

$$\begin{cases} F = F^{(PE)} + F^{(SE)} \\ F^{(CE)} = F^{(SE)} \end{cases} \quad (7)$$

$$\begin{cases} L = L^{(CE)} + L^{(SE)} \\ L = L^{(PE)} \end{cases} \quad (8)$$

The forces are a function of the deformed muscle length according to empirical constants and of the peak isometric force. Moreover, the contractile force ($F^{(CE)}$) depends also on the muscle velocity and activation law. The latter ($a(t)$) is usually determined experimentally [73] or by solving the first-order ordinary differential equation indicated in (9):

$$\frac{da(t)}{dt} = \frac{1}{\tau_{rise}}(1 - a(t))u(t) + \frac{1}{\tau_{fall}}(a_{min} - a(t))(1 - u(t)) \quad (9)$$

where τ_{rise} and τ_{fall} are the time constants, respectively, for the activation and deactivation of the muscles, whereas $u(t)$ is the neural excitation included in the range [0, 1]. The activation function instead goes from a_{min} to 1 [74]. The set of obtained equations is strictly non-linear, inducing complications in their computational resolution. Nevertheless, in hypothesizing a small strain, the governing relationships can be suitably linearized, as applied to the biomechanics of the human tongue by Kajee et al. [75].

In conclusion, FEM modeling for the mechanical properties of soft tissues is somewhat complex due to their nonlinear response. The definition of the muscle features significantly influences the results [76], and it thus is indispensable for a complete and correct description of the biomechanical behavior of the human jaw. To achieve this, the modeling should mimic the human body structure as much as possible [77]. On the other hand, the muscle properties are strictly variable and affected by their functional demands [78]. An interesting procedure for calculating them was proposed by Silva et al. [79] using inverse finite element analysis. The approach provided consistent results with the experimental trials conducted using dynamic magnetic resonance imaging, commonly used in the dental field [80]. In this regard, hyperelastic theory [81], transversely isotropic [82,83] or anisotropic [84–86], was found to be in a good agreement with the experiments, as confirmed by Ferreira et al. [87]. The hyperelasticity of a material is characterized by nonlinear elastic behavior but also described by a strain energy function like the Mooney–Rivlin model [88], which is usually adopted in numerical investigations, as done by Röhrle and Pullan [89] and by Aoun et al. [90].

3. The Literature's Main Results

The screening process (Figure 6) involved three databases, Scopus, Google Scholar and PubMed, and was conducted using these keywords: modelling biomechanics [OR]

multibody biomechanics [AND] maxilla [OR] mandible [OR] jaw. The number of papers examined was 220, divided into 100 from Scopus, 70 from Google Scholar and 50 from PubMed. From this list, 198 were excluded due to not matching the inclusion criteria articulated according to four conditions: indexed papers (n°3), works written in Native English (n°2), analyses of the human mandible (n°50) and computational investigations (n°143). Finally, 22 works were analyzed and discussed. Table 1, beyond including the authors and the titles, highlights the kind of analysis, the aim of the research and the year.

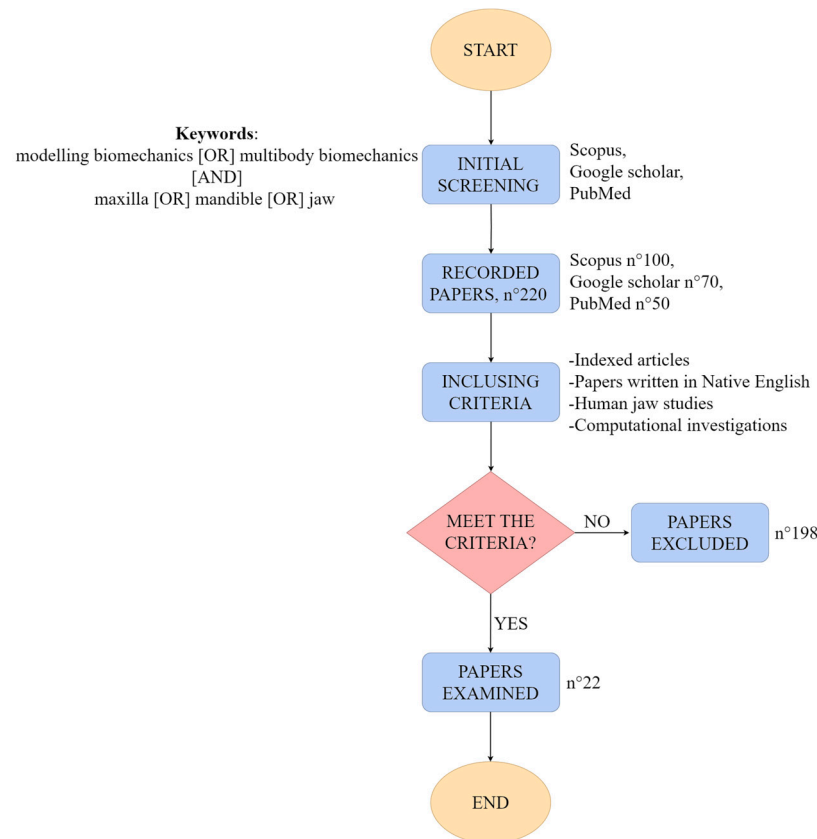


Figure 6. Screening flow chart of literature works.

Table 1. Human jaw biomechanics computational investigations in chronological order.

Number	Authors	Title	Kind of Analysis	Aim	Year
1	Korioth and Hannam [91]	Effect of bilateral asymmetric tooth clenching on load distribution at the mandibular condyles	Dynamics analysis	Evaluation of temporomandibular reaction forces in clenching	1990
2	Ferrario and Sforza [92]	Biomechanical model of the human mandible in unilateral clench: distribution of temporomandibular joint reaction forces between working and balancing sides	Dynamics analysis	Calculation of temporomandibular reaction forces in unilateral clenching	1994
3	Koolstra and Eijden [93]	Dynamics of the human masticatory muscles during a jaw open-close movement	Dynamics model	Analysis of muscle length, velocity and force during mandible opening and closing	1997
4	Langenbach and Hannam [94]	The role of passive muscle tensions in a three-dimensional dynamic model of the human jaw	Dynamics model	Forecast of active and passive jaw muscles	1999

Table 1. Cont.

Number	Authors	Title	Kind of Analysis	Aim	Year
5	Peck et al. [95]	Dynamic simulation of muscle and articular properties during human wide jaw opening	Dynamics model	Analysis of jaw dynamics during a wide opening task	2000
6	Kuboki et al. [96]	Biomechanical calculation of human TM joint loading with jaw opening	Dynamics model	Calculation of muscular and TMJ forces during jaw opening	2000
7	Koolstra and Eijden [97]	Combined finite-element and rigid-body analysis of human jaw joint dynamics	Rigid-body and finite element analysis	Study of stress and deformations of the jaw's cartilaginous structures	2005
8	Choi et al. [98]	Three-dimensional modelling and finite element analysis of the human mandible during clenching	Finite element analysis	Development of a 3D mandible model	2005
9	Hannam et al. [99]	A dynamic model of jaw and hyoid biomechanics during chewing	Forward dynamics analysis of jaw	Prediction of the activation profiles of muscle forces, the loads and the jaw gapes of the condyles during unilateral chewing	2008
10	Bonnet et al. [100]	Biomechanical study of mandible bone supporting a four-implant retained bridge Finite element analysis of the influence of bone anisotropy and foodstuff position	Finite element analysis	Investigation of the biomechanical response of an "All-on-Four" structure	2009
11	Tuijt et al. [101]	Differences in loading of the temporomandibular joint during opening and closing of the jaw	Dynamics analysis	Calculation of reaction forces during opening and closing of the jaw	2010
12	Xiangdong et al. [102]	The influence of the closing and opening muscle groups of jaw condyle biomechanics after mandible bilateral sagittal split ramus osteotomy	Finite Element Analysis	Study of the stress/strain field to assess the impact of jaw opening/closing muscles	2012
13	Ahn et al. [103]	Analyzing center of rotation during opening and closing movements of the mandible using computer simulations	Kinematics analysis	Evaluation of the position of the center of rotation	2015
14	Commisso et al. [104]	Finite element analysis of the human mastication cycle	Finite element analysis	Analysis of stress in the TMJ and of mandible movement for different lateral pterygoid activation patterns	2015
15	Pinheiro and Alves [105]	The feasibility of a custom-made endoprosthesis in mandibular reconstruction: Implant design and finite element analysis	Finite element analysis	Validation of a custom-made endoprosthesis	2015
16	Liu et al. [106]	An Investigation of Two Finite Element Modeling Solutions for Biomechanical Simulation Using a Case Study of a Mandibular Bone	Finite element analysis	Comparison of two different solutions for a mandible stress-strain regime	2017
17	Andersen et al. [107]	Introduction to Force-Dependent Kinematics: Theory and Application to Mandible Modeling	Force-dependent kinematics	Introduction to a novel musculoskeletal modeling approach	2017

Table 1. Cont.

Number	Authors	Title	Kind of Analysis	Aim	Year
18	Kober et al. [108]	Mandibular biomechanics after marginal resection: Correspondences of simulated volumetric strain and skeletal resorption	Finite element analysis	Investigation of mandibular biomechanics after marginal mandibulectomy	2019
19	García et al. [109]	3D kinematic mandible model to design mandibular advancement devices for the treatment of obstructive sleep apnea	3D kinematics analysis	Study of kinematic behavior of the mandible for obstructive sleep apnea issues	2020
20	Dutta et al. [110]	Load transfer across a mandible during a mastication cycle: The effects of odontogenic tumour	Finite element analysis	Comparison of stress–strain fields of healthy and diseased mandibles	2020
21	Guo et al. [111]	EMG-assisted forward dynamics simulation of subject-specific mandible musculoskeletal system	Forward-inverse dynamics analysis	Construction of a predictive model of mandible kinematics and dynamics	2022
22	Sagl et al. [112]	The effect of bolus properties on muscle activation patterns and TMJ loading during unilateral chewing	Forward dynamics analysis	Establishment of kinematics, muscle activations and TMJ stress	2024

4. Discussion

One of the first models of jaw mechanics was offered by the duo Koriouth and Hanam [91] in 1990, concerning unilateral clenching on an acrylic shim and natural teeth. Their approach was founded, during an isometric regime, on the equilibrium theory of both translations and rotations among the muscular and reaction forces, explicated according to the condyle and tooth resistances. The first followed the analytical relationship indicated in (10), whereas the last two were the unknown variables.

$$F_M = [X_M \cdot K] \cdot EMG_M \quad (10)$$

in which X_M is the cross-sectional diameter of the muscle and K [N/m²] a constant [113]. Their product provides the weighting factor, whereas EMG_M represents the scaling factor, indicating the ratio of muscle contraction with respect to its maximum response. They noted that the two structures affected differently the load distribution, which was in the range of 100–400 N, and that when the occlusal load moved toward it, the balancing side suffered more than working side for natural teeth, with the opposite for the acrylic resin shim.

Ferrario and Sforza [92] analyzed the mandible biomechanics according to dynamic analysis with the aim of establishing the reaction forces at the condyle sites. To achieve this, the model, explicated in the sagittal and coronal planes, was based again on the mechanical equilibrium principle between the muscular and condylar forces on the working and balancing sides and the biting forces involved in the vertical and rotation movements. On the contrary, the former forces, involving the masseter, medial and superior lateral pterygoid muscles and temporalis, were considered as a percentage of the biting forces. Analogously, the reaction forces, conveniently scaled on the coronal and sagittal planes using, respectively, asymmetry and activity indexes, were calculated as the percentage of the bite force determined using electromyography. The results showed that the balancing-side joint is not always loaded more than the corresponding working-side joint.

Koolstra and Eijden [93] studied the evolution of the muscular length, velocity and force during the opening and the closing of the mouth. This actuation is determined by the

sarcomere's involvement, whose length ($L_s(t)$) was approximated by the authors using the following law:

$$L_s(t) = [L_m(t) - (L_{mi} - L_{fi})] \cdot \left(\frac{L_{si}}{L_{fi}} \right) \quad (11)$$

where $L_m(t)$ is the muscle length at the instant of time t , L_{mi} and L_{fi} the initial muscle and fiber lengths and L_{si} the initial sarcomere length. The force, therefore, can be obtained as a cubic expression as follows:

$$F_L = 0.4128L_s(t)^3 - 4.3957L_s(t)^2 + 14.8003L_s(t) - 15.0515 \quad (12)$$

in which F_L is the force-length factor representing the instantaneous isometric force as a fraction of the maximum force.

On the other hand, the relationship with the sarcomere's shortening velocity ($V_s(t)$) is indicated in (13):

$$F_V = \left\{ \begin{array}{ll} \frac{12.5 - (V_s(t)/2.73)}{12.5 + (V_s(t)/0.49)} & V_s(t) \geq 0 \\ 1.5 - 0.5 \cdot \left\{ \frac{12.5 + V_s(t)/2.73}{12.5 - 2(V_s(t)/0.49)} \right\} & V_s(t) < 0 \end{array} \right\} \quad (13)$$

In conclusion, the passive forces were evaluated using the passive factor F_P with respect again to the maximum force:

$$F_P = 0.0014 \exp \left(6 \cdot \frac{L_s(t) - 2.73}{2.73} \right) \quad (14)$$

They noted that the passive ones were produced to a larger extent by the jaw-closing muscles (masseter, medial pterygoid, temporalis and superior lateral pterygoid) compared to the opening ones (digastric, geniohyoid, mylohyoid, inferior lateral pterygoid). In addition, they were higher during the opening task. The greatest isometric forces, instead, were determined by the jaw-opening muscles. The previous authors were involved in another study [97], in which rigid-body analysis and the FEM were coupled in a MADYMO environment. The model was based on Hill's theory for the superficial, deep anterior and deep posterior masseter; anterior and posterior temporalis; medial pterygoid; superior and inferior lateral pterygoid; digastric; geniohyoid and anterior and posterior mylohyoid muscles. Their contributions were added to the food resistance in the central incisors and right second molars. The joints were made of two deformable articular cartilage layers [114], where the articular disk, connected to the condyle via pairs of inextensible wires, was free to move. They observed that the reaction forces increased proportionally to the muscle activation, significantly impacting the stressed area but not the peak values of the joint. Moreover, the disk experienced more deformation, mainly due to shear stress, with the maxima in the intermediate zone, than the corresponding cartilaginous layers.

Langenbach and Hannam [94] proposed a dynamic approach to evaluating active and passive muscles during daily activities such as chewing. The model, entirely formulated in the ADAMS package, considered the masseter, temporalis, medial and lateral pterygoid and digastric muscles following Hill's theory. Bite points were coupled also with the resisting forces perpendicular to the occlusal plane, represented with the presence of a food bolus, and the reaction loads in the TMJ, capable of performing five movements (three rotations and two translations). The active and passive muscle profiles were thus extracted and the compressive forces in the joint calculated. In this regard, the working and balancing sides showed different responses with respect to the task: in unilateral chewing, the peaks were on the working side, and the opposite was seen during the chopping cycle. The authors, together with Peck [95], also analyzed the jaw dynamics during a wide opening

task. The mechanical system adopted six degrees of freedom and passive (F_P -Equation (15)) and active (Equation (16)) muscle tensions, solved again using the ADAMS tool.

$$F_P = \frac{(e^{(\text{muscle length}/\text{max muscle length}) \cdot \text{exp}} - 1) \cdot (F_{\text{max}} \cdot \text{factor})}{(e^{\text{exp}} - 1)} \quad (15)$$

As a function of the muscle length, maximum passive force and scaling factor.

$$F_A = F_1 \cdot t_1 + F_1 \cdot t_1 + \dots F_n \cdot t_n \quad (16)$$

where F_1 is the highest force lower than the maximum at an instant of time of actuator activity t_1 , and the others are the forces applied at successive time points. The examined active and passive tensions were low, in the range of 1–18 N. Equally, a wide gap configuration determined the greatest compressive TMJ forces.

Kuboki et al. [96], similar to in the previous studies, proposed a numerical approach centered on the static equilibrium, explicated according to three components, x , y and z , between 14 muscular forces (masseter, temporalis, medial and lateral pterygoid, digastric), gravity and the reaction condyle forces at their corresponding time points. More precisely, the former were calculated as the simple sum of the elastic part of the soft tissue (Equation (17)) and the contractile contribution (Equation (18)).

$$EC = \left(\frac{dL}{L_0}\right)^P \cdot Q \cdot PCS \quad (17)$$

in which dL and L_0 are, respectively, the length at the opening and rest positions, Q the elastic modulus, P a factor and PCS the physiological cross-section of the muscle.

$$CC = \left(\frac{IEMG}{IEMG_{\text{max}}}\right) \cdot LTR \cdot K \cdot PCS \quad (18)$$

where $IEMG$ is the normalized integrated electromyography, and LTR and K are two factors indicating the length–tension and muscle–cross-sectional area relations.

Choi et al. [98] constructed a 3D jaw model in which the masseter, temporalis, medial and lateral pterygoid and digastric muscles [115–117] were applied to a precise area of attachment. These loads, coupled with the biting ones, were assumed to be in equilibrium with the reaction forces positioned at the center of the condyle and modeled as spring elements. The stress values were in the range of 0.3–170 MPa, whereas the deformation was in the range of 0.32–0.71 mm, with its peaks in the condylar region. After the simulations, they observed that the compressive forces on the TMJ were in the range of 3–28 N when the jaw was opened from 10 to 40 mm. In this displacement interval, the digastric muscle reached the maximum activation percentage, whereas the medial temporalis showed the highest elongation percentage.

Hannam et al. [99] modeled the cranium and the jaw using computer tomography (CT), considering the temporomandibular joint as a single point positioned at its center constrained by specific surface movements without friction and adopting Hill's theory for the muscle activations of the anterior, middle and posterior temporalis, superior and inferior lateral pterygoid, deep and superficial masseter, medial pterygoid and anterior digastric muscles. In conclusion, the ArtiSynth software (Version 2.0, 2005) was used for the simulations and the fourth-order Runge–Kutta method for the resolution. The numerical tests provided the muscle excitation profiles, with their peak during mouth opening in the inferior lateral pterygoid and sternohyoid muscles, whereas it was during closing in all the elevator muscles. The ipsilateral condyle, instead, presented the greatest reaction forces.

Bonnet et al. [100] studied the biomechanical behavior of “All-on-Four” treatment, when the anisotropy of bone was taken into account. Equally, the structure was coupled with a sphere simulating foodstuff in the molar, canine and incisor positions. The muscles were modeled both using truss and membrane contractile elements, respectively, for the

masseters, temporalis and lateral and medial pterygoids [118]. The main outcomes were the profound influence of bone anisotropy, which cannot be neglected in FEM analyses, and that the molar position significantly stressed the jaw.

Tuijt et al. [101] realized a three-dimensional mathematical model involving 24 Hill's muscles, indicated by the masseter, temporalis, medial and lateral pterygoid, anterior belly digastric, mylohyoid and geniohyoid. In addition, soft tissues, according to their damping coefficients [119]; gravity; bite forces, through the presence of a simplified dentition and joint forces, using an exponential law, were considered. The numerical tests underlined that the maximum reaction forces occurred during the opening (20–50 N) compared to the closing (5–15 N) of the mouth.

Xiangdong et al. [102] evaluated the stress regime of the jaw in four configurations: normal, protruding, after virtual surgery and after ostectomy. The muscle groups were the masseter, temporalis, medial and lateral pterygoid, digastric, mylohyoid and geniohyoid [120]. The condyles, instead governed by only one degree of freedom, determined the rotation around the sagittal plane. The stress distribution was strongly affected by the jaw muscles, above all by the closing ones in all the scenarios, and it had asymmetrical results concerning the condyles.

Ahn et al. [103] involved the following muscle contributions per side—the masseter (deep and superficial), temporalis (anterior, middle and posterior), medial pterygoid, lateral pterygoid (inferior and superior), digastric and mylohyoid (anterior and posterior)—according to Hill's theory [121]. Furthermore, the temporomandibular ligaments were considered spring elements [122]. The center of rotation was thus estimated using ArtiSynth software, determining that the motion was well described by pure rotation, although it was variable during the opening and closing tasks mainly around the condyle and the mandibular ramus.

Commisso et al. [104], adopting the same muscles as Tuijt et al. [101] and using Hill's theory for both active and passive forces [123], together with the viscoelastic behavior of the articular disk [124], calculated the stress–strain field of the TMJ, noting that the most loaded zone was the articular disk, which had the highest stress at the instant of the maximum mastication force. Lastly, the activation pattern of the lateral pterygoid muscle strongly influenced the biomechanical response of the mandible.

Pinheiro and Alves [105] validated a custom-made endoprosthesis made of Titanium Grade V realized to correct mandibular defects. By fixing the condyles in all three directions and by involving the muscular forces of the masseter, temporalis and lateral and medial pterygoid and different biting loads in diverse tooth positions [125], they analyzed the stress–strain regime of the coupling of the mandible–prosthesis. The great similarity of the stress/strain field with respect to the intact mandible and strain values promoting bone health confirmed the reliability of the apparatus.

Liu et al. [106] investigated two kinds of meshing surfaces, parametric and triangular ones. A CT image was meshed according to these two techniques and successively imported into FEM tools. In this environment, after the definition of the bone's mechanical properties, the constraints and loads were applied. In this analysis, the condyles were fixed in the three directions of translation, whereas the muscle forces, referring to the masseter, temporal (anterior and posterior), depressor and medial and lateral pterygoid, were represented as springs with no resistance [126]. Overall, the authors stated that the best choice was the triangular mesh due to the complexity of oral human apparatus.

Andersen et al. [107] introduced a novel musculoskeletal model in the AnyBody tool, also contemplating the presence of kinematic joints, considering their degrees of freedom (DOFs). In further detail, Equation (1) was rewritten as:

$$\left\{ \begin{array}{l} \Phi(q, t) = 0 \\ \Phi^{FDK}(q, t) - \alpha^{FDK}(q, t) = 0 \end{array} \right\} \quad (19)$$

where α^{FDK} represents the new DOFs whose dynamics can be neglected since their small range of movement. Equally, the authors proposed a division between hard constraints,

which must be solved, and soft constraints, which should be solved as much as possible. This division arises from the greater number of experimentally measured DOFs with respect to the modeled ones. This idea thus determines the definition of an optimization problem for a specific scalar objective function (for example, the weighted least square). Successively, the inverse dynamics can be analyzed, for which the muscular, joint and residual forces F^{FDK} are calculated. The algorithm, based on a Newton–Raphson-based approach augmented with a golden section line, is stopped when the value of α^{FDK} makes these forces 0. In conclusion, the ligaments were also included as three non-linear line elements. The comparison with the experimental data confirmed good agreement concerning the kinematics but not for the joint forces, hence why this approach needs further future improvements.

Kober et al. [108] evaluated the strain regime of a patient subjected to hemimandibulectomy 2.5 years after their first resection. The study was conducted by applying rigid constraints corresponding to the TMJ and muscular forces as distributed loads over the attachments in proximity to the masseter (superficial and deep), temporal (frontal, middle and posterior), medial and lateral pterygoid and digastric muscles and the right first molar tooth. They found that the mandible biomechanics after resection is negatively influenced by muscular activity, especially for subjects in good clinical condition.

Garcia et al. [109] evaluated the kinematics of the mandible in order to fix obstructive sleep apnea. Starting with image analysis, achieved using a 3D Vicon system coupled with four cameras, the jaw movements were recorded. By imposing five degrees of freedom, divided into rigid assumptions for both condyles and the incisors (3) and the condyle movements in the glenoid fossa (2), an iterative process was conducted to calculate the position of any point on the human jaw. Finally, the realized 3D model provided more reliable results compared to a 2D model.

Dutta et al. [110] considered the muscular forces of the masseter (deep and superficial), temporalis (anterior, middle, posterior) and medial and inferior lateral pterygoid [127] in three directions, localized in the patched areas on the outer surface of the cortical shell [128] of the mandible. Moreover, the soft tissue layers in proximity to the articular condyle were applied using two blocks, permitting displacements and rotations and providing support to the apparatus at the same time. The simulations highlighted that, as expected, the presence of a tumor induces higher stress and strains, likely causing pathological fractures during daily activities, like eating.

Guo et al. [111] proposed an interesting model in 2022, combining both inverse and forward dynamics: EMG activities and the maxillary plate landmarks acted as the input variables to obtain the activation function and the position of any point on the jaw. Furthermore, 24 muscles (temporalis, masseter, pterygoid and digastric) were considered in accordance with Hill's theory, whose insertion was achieved using a non-rigid iterative closest point algorithm (NICP). Two proportional, integral, and derivative (PID) controllers were applied in order to monitor the potential errors in the posterior temporalis and pterygoid muscles' length and that of the jaw-opening muscles. In conclusion, inverse–forward dynamics simulation was carried out (Equation (5)), taking into account also the effect of the fibrous capsule and the TMJ ligaments. The simulations showed unintentional movements of head–neck coupling, together with the activation profiles of the jaw-opening and lateral pterygoid muscles.

Lastly, Sagl et al. [112] proposed an in silico model developed in the ArtiSynth environment taking into consideration the bones as rigid bodies; the muscles (masseter, temporalis, pterygoid, mylohyoid, geniohyoid, digastric) as actuators, in accordance with Hill's theory, and the TMJ, composed of the articular disk and ligaments, as made up of elastic contact layers [129]. Moreover, the algorithm satisfied following next equation:

$$\min_a \left(w_v \phi_v(a) + \frac{w_a}{2} a^t a + \frac{w_d}{2} |a_{i-1} - a|^2 \right) \quad 0 \leq a \leq 1 \quad (20)$$

Φ_v is the quadratic optimization function between a movement goal and the motion activated by the muscles (motion tracking error). W_v , w_a , w_d represent specific weights and a the vector of the muscle activations. The condyle displacement range on both the chewing and non-chewing sides, with the von Mises stress in the order of 0.5–2 MPa, was calculated for different bolus positions, sizes and stiffness values, noting that the latter had a significant influence on the mandibular joint only in terms of its size and stiffness.

On the whole, the bond between medicine and engineering is more and more clear in the dental field [130,131]. In light of this, biomechanics is a clear example for which a mechanical theoretical background is applied to biological entities, with the aim of improving a patient's clinical condition [132]. The human jaw is an articulated biosystem [133] composed of several entities, such as muscles, ligaments and bones, which are inserted into numerical models using analytical laws. Hence, studying the mandible's biomechanics is certainly a challenging [134] field of bioengineering. Indeed, the complex mechanical behavior of the human jaw [135], such as the definition of the cartilage's properties, the numerical instabilities [136] and the complexities of anatomic tissue description [137], determine the realization of models with variable grades of limitations [138]. Nevertheless, the development of new technologies and software [139] in recent years has allowed for much deeper investigations, with the aim of correlating rigorously the muscle forces and human tasks such as eating, speaking and so on [140]. In light of this, purely muscular factors like the muscle and fiber length and the pennation angle play a key role in the correct execution of a specific action [141], hence why advanced algorithms capable of modeling muscular and joint interactions have been proposed since the beginning of 21st century [142,143]. For instance, a useful approach may be represented in the combination of different tools, as carried out by Koolstra et al. [97], in terms of coupling multibody analysis with the FEM [144]. On the other hand, computational modeling, essentially based on Hill's theory, requires, most of the time, experimental data as input in order to perform numerical tests [145]. This confirms the requirement for both numerical and experimental but also clinical trials to validate the results obtained. In conclusion, it is most evident that further studies are absolutely required in order to strengthen the current knowledge in this very fascinating field.

5. Conclusions

In this review, computational approaches were considered, mainly involving kinematics, forward and inverse and finite element analyses. Several models of muscular and joint contributions were thus discussed, with their respective hypotheses. The scientific progress made using numerical methodologies, coupled with their non-invasive character and real-time response, confirmed their uncontested success. The current state of the art proposes several different approaches for the estimation of the jaw's muscular and condylar forces in terms of the degrees of freedom involved, the type of analysis and boundary conditions imposed, the mandible modeling, the kind of muscles considered and the specific human activity, making comparison of the results a formidable task. Nevertheless, interesting outcomes were clearly reported in the literature, such as the activation profiles and stress–strain regime explicated in the oral cavity. Moreover, numerical simulations have highlighted the asymmetry between the working and balancing sides and that the presence of any disease, like tumors, induces more stress in the human jaw. Overall, mandible biomechanics is, at the moment, still an open field, with many questions to answer and issues to resolve.

Author Contributions: Conceptualization, M.D.S. and A.R.; literature review, M.D.S.; writing—original draft preparation, M.D.S.; writing—review and editing, M.D.S. and A.R.; supervision, A.R. All authors have read and agreed to the published version of the manuscript.

Funding: This research received no external funding.

Institutional Review Board Statement: Not applicable.

Informed Consent Statement: Not applicable.

Conflicts of Interest: The authors declare no conflicts of interest.

References

- Picasso, B. *Fondamenti di Meccanica e Biomeccanica*; Springer: Milan, Italy, 2012.
- Ruggiero, A.; De Stefano, M.; Rao, T.V.V. Squeaking in Total Hip Arthroplasty. In *Industrial Tribology*; CRC Press: Boca Raton, FL, USA, 2022.
- Madeti, B.K.; Chalamalasetti, S.R.; Pragada, S.K.S. Biomechanics of knee joint—A review. *Front. Mech. Eng.* **2015**, *10*, 176–186.
- Czerniecki, J.M. Foot and ankle biomechanics in walking and running: A review. *Am. J. Phys. Med. Rehabil.* **1988**, *67*, 246–252.
- Ruggiero, A.; De Stefano, M. Experimental Investigation on the Bio-tribocorrosive behavior of Ti6Al4V alloy and 316 L stainless steel in two biological solutions. *Tribol. Int.* **2023**, *190*, 109033. [[CrossRef](#)]
- Ruggiero, A.; De Stefano, M. On the Biotribological Surfaces of Dental Implants: Investigation in the Framework of Osseointegration. *Biotribology* **2023**, *35–36*, 100254. [[CrossRef](#)]
- De Stefano, M.; Aliberti, S.M.; Ruggiero, A. (Bio)Tribocorrosion in Dental Implants: Principles and Techniques of Investigation. *Appl. Sci.* **2022**, *12*, 7421. [[CrossRef](#)]
- Lanza, A.; De Stefano, M.; Ruggiero, A. Investigating the optimal design of All-on-Four technique adopting finite element analysis: The aspect of framework material, kind and position of implants. *Biomed. Eng. Adv.* **2023**, *6*, 100110.
- De Stefano, M.; Lanza, A.; Faia, E.; Ruggiero, A. A novel ultrashort dental implant design for the reduction of the bone stress/strain: A comparative numerical investigation. *Biomed. Eng. Adv.* **2023**, *5*, 100077. [[CrossRef](#)]
- De Stefano, M.; Lanza, A.; Sbordone, L.; Ruggiero, A. Stress-strain and fatigue life numerical evaluation of two different dental implants considering isotropic and anisotropic human jaw. *Proc. Inst. Mech. Eng. Part H J. Eng. Med.* **2023**, *237*, 1190–1201. [[CrossRef](#)]
- Smith, A.L.; Davis, J.; Panagiotopoulou, O.; Taylor, A.B.; Robinson, C.; Ward, C.V.; Kimbel, W.H.; Alemseged, Z.; Ross, C.F. Does the model reflect the system? When two-dimensional biomechanics is not ‘good enough’. *J. R. Soc. Interface* **2023**, *20*, 20220536. [[CrossRef](#)]
- Teixeira, E.R.; Sato, Y.; Akagawa, Y.; Shindoi, S. A comparative evaluation of mandibular finite element models with different lengths and elements for implant biomechanics. *J. Oral Rehabil.* **1998**, *25*, 299–303. [[CrossRef](#)]
- Anitua, E.; Ibarra, N.L.S.; Rotaecche, L.S. Implant-Supported Prosthesis in the Edentulous Mandible: Biomechanical Analysis of Different Implant Configurations via Finite Element Analysis. *Dent. J.* **2023**, *11*, 4. [[CrossRef](#)] [[PubMed](#)]
- Ichim, I.; Swain, M.V.; Kieser, J.A. Mandibular stiffness in humans: Numerical predictions. *J. Biomech.* **2006**, *39*, 1903–1913. [[CrossRef](#)]
- Ansoms, P.; Barzegari, M.; Sloten, J.V.; Geris, L. Coupling biomechanical models of implants with biodegradation models: A case study for biodegradable mandibular bone fixation plates. *J. Mech. Behav. Biomed. Mater.* **2023**, *147*, 106120. [[CrossRef](#)]
- Balshi, T.J.; Wolfinger, G.J.; Stein, B.E.; Balshi, S.F. A long-term retrospective analysis of survival rates of implants in the mandible. *Int. J. Oral Maxillofac. Implants* **2015**, *30*, 1348–1354. [[CrossRef](#)]
- Khadembaschi, D.; Brierly, G.I.; Chatfield, M.D.; Beech, N.; Batstone, M.D. Systematic review and pooled analysis of survival rates, success, and outcomes of osseointegrated implants in a variety of composite free flaps. *Head Neck* **2020**, *42*, 2669–2686. [[CrossRef](#)]
- Vollmer, D.; Meyer, U.; Joos, U.; Vègh, A.; Piffko, J. Experimental and finite element study of a human mandible. *J. Craniomaxillofac. Surg.* **2000**, *28*, 91–96. [[CrossRef](#)]
- Viano, D.C.; Bir, C.; Walilko, T.; Sherman, D. Ballistic Impact to the Forehead, Zygoma, and Mandible: Comparison of Human and Frangible Dummy Face Biomechanics. *J. Trauma Inj. Infect. Crit. Care* **2004**, *56*, 1305–1311. [[CrossRef](#)]
- Bujtár, P.; Simonovics, J.; Váradi, K.; Sándor, G.K.B.; Avery, C.M.E. The biomechanical aspects of reconstruction for segmental defects of the mandible: A finite element study to assess the optimisation of plate and screw factors. *J. Cranio-Maxillofac. Surg.* **2014**, *42*, 855–862. [[CrossRef](#)]
- Alkan, A.; Celebi, N.; Ozden, B.; Baş, B.; Inal, S. Biomechanical comparison of different plating techniques in repair of mandibular angle fractures. *Oral Surg. Oral Med. Oral Pathol. Oral Radiol. Endod.* **2007**, *104*, 752–756. [[CrossRef](#)]
- Ingawalé, S.; Goswami, T. Temporomandibular Joint: Disorders, Treatments, and Biomechanics. *Ann. Biomed. Eng.* **2009**, *37*, 976–996. [[CrossRef](#)]
- Zhong, S.; Shi, Q.; Sun, Y.; Yang, S.; Dessel, V.J.; Gu, Y.; Chen, X.; Lübbers, H.-T.; Politis, C. Biomechanical comparison of locking and non-locking patient-specific mandibular reconstruction plate using finite element analysis. *J. Mech. Behav. Biomed. Mater.* **2021**, *124*, 104849. [[CrossRef](#)] [[PubMed](#)]
- Bezerra, T.P.; Junior, F.I.S.; Scarparo, H.C.; Costa, F.W.G.; Studart-Soares, E.C. Do erupted third molars weaken the mandibular angle after trauma to the chin region? A 3D finite element study. *Int. J. Oral Maxillofac. Surg.* **2013**, *42*, 474–478. [[CrossRef](#)] [[PubMed](#)]
- Antic, S.; Vukicevic, A.M.; Milasinovic, M.; Saveljic, I.; Jovicic, G.; Filipovic, N.; Rakocevic, Z.; Djuric, M. Impact of the lower third molar presence and position on the fragility of mandibular angle and condyle: A Three-dimensional finite element study. *J. Craniomaxillofac. Surg.* **2015**, *43*, 870–878. [[CrossRef](#)] [[PubMed](#)]

26. Huys, S.E.F.; Keelson, B.; Brucker, Y.; Gompel, G.V.; Mey, J.; Sloten, J.V.; Buls, N. The use of dynamic CT imaging for tracking mandibular movements in a phantom. *Biomed. Phys. Eng. Express* **2022**, *9*, 015002. [[CrossRef](#)] [[PubMed](#)]
27. Christensen, L.V.; Rassouli, N.M. Experimental occlusal interferences. Part I. A review. *J. Oral Rehabil.* **1995**, *22*, 515–520. [[CrossRef](#)]
28. Cheng, K.J.; Liu, Y.F.; Wang, J.H.; Jun, J.C.; Jiang, X.F.; Wang, R.; Baur, D.A. Biomechanical behavior of mandibles reconstructed with fibular grafts at different vertical positions using finite element method. *J. Plast. Reconstr. Aesthet. Surg.* **2019**, *72*, 281–289. [[CrossRef](#)] [[PubMed](#)]
29. Pepicelli, A.; Woods, M.; Briggs, C. The mandibular muscles and their importance in orthodontics: A contemporary review. *Am. J. Orthod. Dentofac. Orthop.* **2005**, *128*, 774–780. [[CrossRef](#)] [[PubMed](#)]
30. Pinheiro, M.; Willaert, R.; Khan, A.; Krairi, A.; Paepegem, W.V. Biomechanical evaluation of the human mandible after temporomandibular joint replacement under different biting conditions. *Sci. Rep.* **2021**, *11*, 14034. [[CrossRef](#)] [[PubMed](#)]
31. Meyer, C.; Kahn, J.L.; Lambert, A.; Boutemy, P.; Wilk, A. Development of a static simulator of the mandible. *J. Cranio-Maxillofac. Surg.* **2000**, *28*, 278–286. [[CrossRef](#)]
32. Choi, A.H.; Conway, R.C.; Taraschi, V.; Ben-Nissan, B. Biomechanics and functional distortion of the human mandible. *J. Investig. Clin. Dent.* **2015**, *6*, 241–251. [[CrossRef](#)]
33. Curtis, D.A.; Plesh, O.; Hannam, A.G.; Sharma, A.; Curtis, T.A. Modeling of jaw biomechanics in the reconstructed mandibulectomy patient. *J. Prosthet. Dent.* **1999**, *81*, 167–173. [[CrossRef](#)] [[PubMed](#)]
34. Ahlgren, J.; Öwall, B. Muscular activity and chewing force: A polygraphic study of human mandibular movements. *Arch. Oral Biol.* **1970**, *15*, 271–280. [[CrossRef](#)]
35. Hiraba, K.; Hibino, K.; Hiranuma, K.; Negoro, T. EMG activities of two heads of the human lateral pterygoid muscle in relation to mandibular condyle movement and biting force. *J. Neurophysiol.* **2000**, *83*, 2120–2137. [[CrossRef](#)] [[PubMed](#)]
36. Saini, H.; Ackland, D.C.; Gong, L.; Cheng, L.K.; Röhrle, O. Occlusal load modelling significantly impacts the predicted tooth stress response during biting: A simulation study. *Comput. Methods Biomech. Biomed. Eng.* **2020**, *23*, 261–270. [[CrossRef](#)] [[PubMed](#)]
37. Shi, Q.; Sun, Y.; Yang, S.; Dessel, J.V.; Lübbers, H.T.; Zhong, S.; Gu, Y.; Bila, M.; Politis, C. Preclinical study of additive manufactured plates with shortened lengths for complete mandible reconstruction: Design, biomechanics simulation, and fixation stability assessment. *Comput. Biol. Med.* **2021**, *139*, 105008. [[CrossRef](#)] [[PubMed](#)]
38. Koriath, T.W.; Romilly, D.P.; Hannam, A.G. Three-dimensional finite element stress analysis of the dentate human mandible. *Am. J. Phys. Anthropol.* **1992**, *88*, 69–96. [[CrossRef](#)] [[PubMed](#)]
39. Koriath, T.W.; Hannam, A.G. Deformation of the human mandible during simulated tooth clenching. *J. Dent. Res.* **1994**, *73*, 56–66. [[CrossRef](#)] [[PubMed](#)]
40. Naeije, M.; Hofman, N. Biomechanics of the human temporomandibular joint during chewing. *J. Dent. Res.* **2003**, *82*, 528–531. [[CrossRef](#)] [[PubMed](#)]
41. Yachouh, J.; Domergue, S.; Hoarau, R.; Loosli, Y.; Goudot, P. Biomechanics of the weakened mandible: Use of image correlation analysis. *Br. J. Oral Maxillofac. Surg.* **2013**, *51*, e137–e141. [[CrossRef](#)]
42. Prasad, S.; Suresh, S.; Hong, K.L.; Bhargava, A.; Rosa, V.; Wong, R.C.W. Biomechanics of alloplastic mandible reconstruction using biomaterials: The effect of implant design on stress concentration influences choice of material. *J. Mech. Behav. Biomed. Mater.* **2020**, *103*, 103548. [[CrossRef](#)]
43. Ramos, A.; Ballu, A.; Mesnard, M.; Talaia, P.; Simões, J.A. Numerical and Experimental Models of the Mandible. *Exp. Mech.* **2011**, *51*, 1053–1059. [[CrossRef](#)]
44. Knoell, A.C. A mathematical model of an in vitro human mandible. *J. Biomech.* **1977**, *10*, 159–166. [[CrossRef](#)]
45. Ichim, I.; Swain, M.; Kieser, J.A. Mandibular biomechanics and development of the human chin. *J. Dent. Res.* **2006**, *85*, 638–642. [[CrossRef](#)] [[PubMed](#)]
46. Aftabi, H.; Zaraska, K.; Eghbal, A.; McGregor, S.; Prisman, E.; Hodgson, A.; Fels, S. Computational models and their applications in biomechanical analysis of mandibular reconstruction surgery. *Comput. Biol. Med.* **2023**, *169*, 107887. [[CrossRef](#)]
47. Natali, A.N.; Carniel, E.L.; Pavan, P.G. Modelling of mandible bone properties in the numerical analysis of oral implant biomechanics. *Comput. Methods Programs Biomed.* **2010**, *100*, 158–165. [[CrossRef](#)]
48. Craig, M.; Bir, C.; Viano, D.; Tashman, S. Biomechanical response of the human mandible to impacts of the chin. *J. Biomech.* **2008**, *41*, 2972–2980. [[CrossRef](#)]
49. Alvarez-Arenal, A.; Lasheras, F.S.; Fernández, E.M.; González, I. A jaw model for the study of the mandibular flexure taking into account the anisotropy of the bone. *Math. Comput. Model.* **2009**, *50*, 695–704. [[CrossRef](#)]
50. Meira, J.B.C.; Landgraf, H.; Shinohara, E.H.; Luz, J.G.C.; Ballester, R.Y. A new way of evaluating the biomechanics of the mandible with freedom in three axes in space: Technical note. *J. Oral Maxillofac. Surg. Med. Pathol.* **2018**, *30*, 405–408. [[CrossRef](#)]
51. Santis, R.D.; Mollica, F.; Esposito, R.; Ambrosio, L.; Nicolais, L. An experimental and theoretical composite model of the human mandible. *J. Mater. Sci. Mater. Med.* **2005**, *16*, 1191–1197. [[CrossRef](#)] [[PubMed](#)]
52. Wong, R.C.W.; Tideman, H.; Kin, L.; Merckx, M.A.W. Biomechanics of mandibular reconstruction: A review. *Int. J. Oral Maxillofac. Surg.* **2010**, *39*, 313–319. [[CrossRef](#)] [[PubMed](#)]
53. Bedrossian, E.; Bedrossian, E.A. Treatment Planning the Edentulous Mandible. Review of Biomechanical and Clinical Considerations: An Update. *Int. J. Oral Maxillofac. Implant.* **2019**, *34*, e33. [[CrossRef](#)] [[PubMed](#)]
54. Eijden, T.M. Biomechanics of the Mandible. *Crit. Rev. Oral Biol. Med.* **2000**, *11*, 123–136. [[CrossRef](#)] [[PubMed](#)]

55. Roberts, W.E.; Goodacre, C.J. The Temporomandibular Joint: A Critical Review of Life-Support Functions, Development, Articular Surfaces, Biomechanics and Degeneration. *J. Prosthodont.* **2020**, *29*, 772–779. [[CrossRef](#)] [[PubMed](#)]
56. Wong, R.C.W.; Tideman, H.; Merckx, M.A.W.; Jansen, J.; Goh, S.M.; Liao, K. Review of biomechanical models used in studying the biomechanics of reconstructed mandibles. *Int. J. Oral Maxillofac. Surg.* **2011**, *40*, 393–400. [[CrossRef](#)]
57. Gupta, K.K.; Knoell, A.C.; Grenoble, D.E. Mathematical modeling and structural analysis of the mandible. *Biomater. Med. Devices Artif. Organs* **1973**, *1*, 469–479. [[CrossRef](#)]
58. Hannam, A.G. Dynamic modeling and jaw biomechanics. *Orthod. Craniofac. Res.* **2003**, *1*, 59–65. [[CrossRef](#)] [[PubMed](#)]
59. Vallabh, R.; Zhang, J.; Fernandez, J.; Dimitroulis, G.; Ackland, D.C. The morphology of the human mandible: A computational modelling study. *Biomech. Model. Mechanobiol.* **2020**, *19*, 1187–1202. [[CrossRef](#)]
60. Li, P.; Tang, Y.; Li, J.; Shen, L.; Tian, W.; Tang, W. Establishment of sequential software processing for a biomechanical model of mandibular reconstruction with custom-made plate. *Comput. Methods Programs Biomed.* **2013**, *111*, 642–649. [[CrossRef](#)]
61. Liao, S.H.; Tong, R.F.; Dong, J.X. Influence of anisotropy on peri-implant stress and strain in complete mandible model from CT. *Comput. Med. Imaging Graph.* **2008**, *32*, 53–60. [[CrossRef](#)]
62. Tomonari, H.; Kwon, S.; Kuninori, T.; Miyawaki, S. Differences between the chewing and non-chewing sides of the mandibular first molars and condyles in the closing phase during chewing in normal subjects. *Arch. Oral Biol.* **2017**, *81*, 198–205. [[CrossRef](#)]
63. Baba, K.; Yugami, K.; Yaka, T.; Ai, M. Impact of balancing-side tooth contact on clenching induced mandibular displacements in humans. *J. Oral Rehabil.* **2001**, *28*, 721–727. [[CrossRef](#)]
64. Visscher, C.M.; Slater, J.J.R.H.; Lobbezoo, F.; Naeije, M. Kinematics of the human mandible for different head postures. *J. Oral Rehabil.* **2000**, *27*, 299–305. [[CrossRef](#)]
65. Ambrósio, J.A.C.; Kecskeméthy, A. Multibody Dynamics of Biomechanical Models for Human Motion via Optimization. In *Computational Methods in Applied Sciences*; Springer: Berlin/Heidelberg, Germany, 2007; pp. 245–272.
66. Winters, J.M. Hill-Based Muscle Models: A Systems Engineering Perspective. In *Multiple Muscle Systems*; Springer: Berlin/Heidelberg, Germany, 1990; pp. 69–93.
67. Siebert, T.; Rode, C.; Herzog, W.; Till, O.; Blickhan, R. Nonlinearities make a difference: Comparison of two common Hill-type models with real muscle. *Biol. Cybern.* **2008**, *98*, 133–143. [[CrossRef](#)] [[PubMed](#)]
68. Carbone, V.; Krogt, M.M.d.; Koopman, H.F.J.M.; Verdonschot, N. Sensitivity of subject-specific models to Hill muscle–tendon model parameters in simulations of gait. *J. Biomech.* **2016**, *49*, 1953–1960. [[CrossRef](#)]
69. Cansız, B.; Dal, H.; Kaliske, M. Computational cardiology: A modified Hill model to describe the electro-visco-elasticity of the myocardium. *Comput. Methods Appl. Mech. Eng.* **2017**, *315*, 434–466. [[CrossRef](#)]
70. Hill, A.V. The heat of shortening and the dynamic constants of muscle. *Proc. R. Soc. Biol.* **1938**, *126*, 136–195.
71. Hill, A.V. The mechanics of active muscle. *Proc. R. Soc. Lond. Ser. B Biol. Sci.* **1953**, *141*, 104–117.
72. Martins, J.A.C.; Pires, E.B.; Salvado, R.; Dinis, P.B. A numerical model of passive and active behavior of skeletal muscles. *Comput. Methods Appl. Mech. Eng.* **1998**, *151*, 419–433. [[CrossRef](#)]
73. Strobach, D.; Kecskeméthy, A.; Steinwender, G.; Zwick, E.B. Rapid identification of muscle activation profiles via optimization and smooth profile patches. *Mater. Sci. Eng. Technol.* **2005**, *36*, 802–813.
74. Martins, J.A.C.; Pato, M.P.M.; Pires, E.B. A finite element model of skeletal muscles. *Virtual Phys. Prototyp.* **2007**, *1*, 159–170. [[CrossRef](#)]
75. Kajee, Y.; Pelteret, J.P.V.; Reddy, B.D. The biomechanics of the human tongue. *Int. J. Numer. Methods Biomed. Eng.* **2013**, *29*, 492–514. [[CrossRef](#)]
76. Strait, D.S.; Wang, Q.; Dechow, P.C.; Ross, C.F.; Richmond, B.G.; Spencer, M.A.; Patel, B.A. Modeling elastic properties in finite-element analysis: How much precision is needed to produce an accurate model? *Anat. Rec.* **2005**, *283*, 275–287. [[CrossRef](#)]
77. Zhen, T.; Zhonghua, Z.; Gang, Z.; Yubin, C.; Tao, L.; Yinghui, T. Establishment of a three-dimensional finite element model for gunshot wounds to the human mandible. *J. Med. Coll. PLA* **2012**, *27*, 87–100. [[CrossRef](#)]
78. Grünheid, T.; Langenbach, G.E.J.; Korfage, J.A.M.; Zentner, A.; Eijden, T.M.G.J. The adaptive response of jaw muscles to varying functional demands. *Eur. J. Orthod.* **2009**, *31*, 596–612. [[CrossRef](#)]
79. Silva, M.; Brandão, S.; Parente, M.P.L.; Mascarenhas, T.; Jorge, R.M.N. Establishing the biomechanical properties of the pelvic soft tissues through an inverse finite element analysis using magnetic resonance imaging. *Proc. Inst. Mech. Eng. Part H J. Eng. Med.* **2016**, *230*, 298–309. [[CrossRef](#)]
80. Hannam, A.G.; Wood, W.W. Relationships between the size and spatial morphology of human masseter and medial pterygoid muscles, the craniofacial skeleton, and jaw biomechanics. *Am. J. Biol. Anthropol.* **1989**, *80*, 429–445. [[CrossRef](#)]
81. Hamma, A.; Boisson, J.; Serantoni, V.; Dallard, J. Identification of a visco-hyperelastic model for mandibular periosteum. *J. Mech. Behav. Biomed. Mater.* **2022**, *133*, 105323. [[CrossRef](#)]
82. Kulkarni, S.G.; Gao, X.L.; Horner, S.E.; Mortlock, R.F.; Zheng, J.Q. A transversely isotropic visco-hyperelastic constitutive model for soft tissues. *Math. Mech. Solids* **2014**, *21*, 748–770. [[CrossRef](#)]
83. Limbert, G.; Middleton, J. A transversely isotropic viscohyperelastic material: Application to the modeling of biological soft connective tissues. *Int. J. Solids Struct.* **2004**, *41*, 4237–4260. [[CrossRef](#)]
84. Chaimoon, K.; Chindaprasirt, P. An anisotropic hyperelastic model with an application to soft tissues. *Eur. J. Mech.-A/Solids* **2019**, *78*, 103845. [[CrossRef](#)]

85. Castillo-Méndez, C.; Ortiz, A. Role of anisotropic invariants in numerically modeling soft biological tissues as transversely isotropic hyperelastic materials: A comparative study. *Int. J. Non-Linear Mech.* **2022**, *138*, 103833. [[CrossRef](#)]
86. Nolan, D.R.; Gower, A.L.; Destrade, M.; Ogden, R.W.; McGarry, J.P. A robust anisotropic hyperelastic formulation for the modelling of soft tissue. *J. Mech. Behav. Biomed. Mater.* **2014**, *39*, 48–60. [[CrossRef](#)]
87. Ferreira, J.P.S.; Parente, M.P.L.; Jabareen, M.; Jorge, R.M.N. A general framework for the numerical implementation of anisotropic hyperelastic material models including non-local damage. *Biomech. Model. Mechanobiol.* **2017**, *16*, 1119–1140. [[CrossRef](#)] [[PubMed](#)]
88. Choy, S.E.M.; Lenz, J.; Schweizerhof, K.; Schmitter, M.; Schindler, H.J. Realistic kinetic loading of the jaw system during single chewing cycles: A finite element study. *J. Oral Rehabil.* **2017**, *44*, 375–384. [[CrossRef](#)]
89. Röhrle, O.; Pullan, A.J. Three-dimensional finite element modelling of muscle forces during mastication. *J. Biomech.* **2007**, *40*, 3363–3372. [[CrossRef](#)]
90. Aoun, M.; Mesnard, M.; Monède-Hocquard, L.; Ramos, A. Stress Analysis of Temporomandibular Joint Disc During Maintained Clenching Using a Viscohyperelastic Finite Element Model. *J. Oral Maxillofac. Surg.* **2014**, *72*, 1070–1077. [[CrossRef](#)] [[PubMed](#)]
91. Korioth, W.T.; Hannam, A.G. Effect of bilateral asymmetric tooth clenching on load distribution at the mandibular condyles. *J. Prosthet. Dent.* **1990**, *64*, 62–73. [[CrossRef](#)]
92. Ferrario, V.F.; Sforza, C. Biomechanical model of the human mandible in unilateral clench: Distribution of temporomandibular joint reaction forces between working and balancing sides. *J. Prosthet. Dent.* **1994**, *72*, 169–176. [[CrossRef](#)]
93. Koolstra, J.H.; Eijden, T.M. Dynamics of the human masticatory muscles during a jaw open-close movement. *J. Biomech.* **1997**, *30*, 883–889. [[CrossRef](#)]
94. Langenbach, G.E.J.; Hannam, A.G. The role of passive muscle tensions in a three-dimensional dynamic model of the human jaw. *Arch. Oral Biol.* **1999**, *44*, 557–573. [[CrossRef](#)]
95. Peck, C.C.; Langenbach, G.E.; Hannam, A.G. Dynamic simulation of muscle and articular properties during human wide jaw opening. *Arch. Oral Biol.* **2000**, *45*, 963–982. [[CrossRef](#)] [[PubMed](#)]
96. Kuboki, T.; Takenami, Y.; Maekawa, K.; Shinoda, M.; Yamashita, A.; Clark, G.T. Biomechanical calculation of human TM joint loading with jaw opening. *J. Oral Rehabil.* **2000**, *27*, 940–951. [[CrossRef](#)] [[PubMed](#)]
97. Koolstra, J.H.; Eijden, T.M.G.J. Combined finite-element and rigid-body analysis of human jaw joint dynamics. *J. Biomech.* **2005**, *38*, 2431–2439. [[CrossRef](#)] [[PubMed](#)]
98. Choi, A.H.; Ben-Nissan, B.; Conway, R.C. Three-dimensional modelling and finite element analysis of the human mandible during clenching. *Aust. Dent. J.* **2005**, *50*, 42–48. [[CrossRef](#)] [[PubMed](#)]
99. Hannam, A.G.; Stavness, I.; Lloyd, J.E.; Fels, S. A dynamic model of jaw and hyoid biomechanics during chewing. *J. Biomech.* **2008**, *41*, 1069–1076. [[CrossRef](#)] [[PubMed](#)]
100. Bonnet, A.S.; Postaire, M.; Lipinski, P. Biomechanical study of mandible bone supporting a four-implant retained bridge Finite element analysis of the influence of bone anisotropy and foodstuff position. *Med. Eng. Phys.* **2009**, *31*, 806–815. [[CrossRef](#)] [[PubMed](#)]
101. Tuijt, M.; Koolstra, J.H.; Lobbezoo, F.; Naeije, M. Differences in loading of the temporomandibular joint during opening and closing of the jaw. *J. Biomech.* **2010**, *43*, 1048–1054. [[CrossRef](#)] [[PubMed](#)]
102. Xiangdong, Q.L.; Limin, M.A.; Shizhen, Z. The influence of the closing and opening muscle groups of jaw condyle biomechanics after mandible bilateral sagittal split ramus osteotomy. *J. Craniomaxillofac. Surg.* **2012**, *40*, e159–e164. [[CrossRef](#)] [[PubMed](#)]
103. Ahn, S.J.; Tsou, L.; Sánchez, C.A.; Fels, S.; Kwon, H.B. Analyzing center of rotation during opening and closing movements of the mandible using computer simulations. *J. Biomech.* **2015**, *48*, 666–671. [[CrossRef](#)]
104. Commisso, M.S.; Martínez-Reina, J.; Ojeda, J.; Mayo, J. Finite element analysis of the human mastication cycle. *J. Mech. Behav. Biomed. Mater.* **2015**, *41*, 23–35. [[CrossRef](#)]
105. Pinheiro, M.; Alves, J.L. The feasibility of a custom-made endoprosthesis in mandibular reconstruction: Implant design and finite element analysis. *J. Craniomaxillofac. Surg.* **2015**, *43*, 2116–2128. [[CrossRef](#)] [[PubMed](#)]
106. Liu, Y.F.; Fan, Y.Y.; Dong, H.Y.; Zhang, J.X. An Investigation of Two Finite Element Modeling Solutions for Biomechanical Simulation Using a Case Study of a Mandibular Bone. *J. Biomech. Eng.* **2017**, *139*, 121006. [[CrossRef](#)] [[PubMed](#)]
107. Andersen, M.S.; Zee, M.; Damsgaard, M.; Nolte, D.; Rasmussen, J. Introduction to Force-Dependent Kinematics: Theory and Application to Mandible Modeling. *J. Biomech. Eng.* **2017**, *139*, 091001.
108. Kober, C.; Kjeller, G.; Hellmich, C.; Sader, R.A.; Berg, B.I. Mandibular biomechanics after marginal resection: Correspondences of simulated volumetric strain and skeletal resorption. *J. Biomech.* **2019**, *95*, 109320. [[CrossRef](#)] [[PubMed](#)]
109. García, M.; Cabrera, J.A.; Bataller, A.; Postigo, S.; Castillo, J.J. 3D kinematic mandible model to design mandibular advancement devices for the treatment of obstructive sleep apnea. *Bio-Des. Manuf.* **2021**, *4*, 22–32. [[CrossRef](#)]
110. Dutta, A.; Mukherjee, K.; Seesala, V.S.; Dutta, K.; Paul, R.R.; Dhara, S.; Gupta, S. Load transfer across a mandible during a mastication cycle: The effects of odontogenic tumour. *Proc. Inst. Mech. Eng. Part H* **2020**, *234*, 486–495. [[CrossRef](#)] [[PubMed](#)]
111. Guo, J.; Chen, J.; Wang, J.; Ren, G.; Tian, Q.; Guo, C. EMG-assisted forward dynamics simulation of subject-specific mandible musculoskeletal system. *J. Biomech.* **2022**, *139*, 111143. [[CrossRef](#)] [[PubMed](#)]
112. Sagl, B.; Schmid-Schwap, M.; Piehslinger, E.; Yao, H.; Rausch-Fan, X.; Stavness, I. The effect of bolus properties on muscle activation patterns and TMJ loading during unilateral chewing. *J. Mech. Behav. Biomed. Mater.* **2024**, *151*, 106401. [[CrossRef](#)] [[PubMed](#)]

113. Weijs, W.A.; Hillen, B. Relationship between the physiological cross-section of the human jaw muscles and their cross-sectional area in computer tomograms. *Acta Anat.* **1984**, *118*, 129–138. [[CrossRef](#)]
114. Hansson, T.; Oberg, T.; Carlsson, G.E.; Kopp, S. Thickness of the soft tissue layers and the articular disk in the temporomandibular joint. *Acta Odontol. Scand.* **1977**, *35*, 77–83. [[CrossRef](#)]
115. Barbenel, J.C. The biomechanics of the temporomandibular joint: A theoretical study. *J. Biomech.* **1972**, *5*, 251–256. [[CrossRef](#)] [[PubMed](#)]
116. Throckmorton, G.S. Quantitative calculations of temporomandibular joint reaction forces—II. The importance of the direction of the jaw muscle forces. *J. Biomech.* **1985**, *18*, 453–461. [[CrossRef](#)]
117. Pruijm, G.J.; Jongh, H.J.; Bosch, J.J. Forces acting on the mandible during bilateral static bite at different bite force levels. *J. Biomech.* **1980**, *13*, 755–763. [[CrossRef](#)] [[PubMed](#)]
118. Daas, M.; Dubois, G.; Bonnet, A.S.; Lipinski, P.; Rignon-Bret, C. A complete finite element model of a mandibular implant-retained overdenture with two implants: Comparison between rigid and resilient attachment configurations. *Med. Eng. Phys.* **2008**, *30*, 218–225. [[CrossRef](#)] [[PubMed](#)]
119. Koolstra, J.H.; Eijden, T.M. Biomechanical analysis of jaw-closing movements. *J. Dent. Res.* **1995**, *74*, 1564–1570. [[CrossRef](#)]
120. Koolstra, J.H.; Eijden, T.M.G.v. Prediction of volumetric strain in the human temporomandibular joint cartilage during jaw movement. *J. Anat.* **2006**, *209*, 369–380. [[CrossRef](#)]
121. Zajac, F.E. Muscle and tendon: Properties, models, scaling, and application to biomechanics and motor control. *Crit. Rev. Biomed. Eng.* **1989**, *17*, 359–411.
122. Osborn, J.W. A model to describe how ligaments may control symmetrical jaw opening movements in man. *J. Oral Rehabil.* **1993**, *20*, 585–604. [[CrossRef](#)] [[PubMed](#)]
123. Thelen, D.G. Adjustment of muscle mechanics model parameters to simulate dynamic contractions in older adults. *J. Biomech. Eng.* **2003**, *125*, 70–77. [[CrossRef](#)]
124. Comisso, M.S.; Martínez-Reina, J.; Mayo, J. A study of the temporomandibular joint during bruxism. *Int. J. Oral Sci.* **2014**, *6*, 116–123. [[CrossRef](#)]
125. Ferrario, V.F.; Sforza, C.; Serrao, G.; Dellavia, C.; Tartaglia, G.M. Single tooth bite forces in healthy young adults. *J. Oral Rehabil.* **2004**, *31*, 18–22. [[CrossRef](#)] [[PubMed](#)]
126. Hart, R.T.; Hennebel, V.V.; Thongpreda, N.; Buskirk, W.C.V.; Anderson, R.C. Modeling the biomechanics of the mandible: A three-dimensional finite element study. *J. Biomech.* **1992**, *25*, 261–286. [[CrossRef](#)] [[PubMed](#)]
127. Koriotoh, T.W.; Hannam, A.G. Mandibular forces during simulated tooth clenching. *J. Orofac. Pain* **1994**, *8*, 178–189. [[PubMed](#)]
128. Hijazi, L.; Hejazi, W.; Darwich, M.A.; Darwich, K. Finite element analysis of stress distribution on the mandible and condylar fracture osteosynthesis during various clenching tasks. *Oral Maxillofac. Surg.* **2016**, *20*, 359–367. [[CrossRef](#)] [[PubMed](#)]
129. Blankevoort, L.; Kuiper, J.H.; Huiskes, R.; Grootenboer, H.J. Articular contact in a three-dimensional model of the knee. *J. Biomech.* **1991**, *24*, 1019–1031. [[CrossRef](#)] [[PubMed](#)]
130. Weng, Y.; Cao, Y.; Arevalo, C.; Vacanti, M.P.; Vacanti, C.A. Tissue-engineered composites of bone and cartilage for mandible condylar reconstruction. *J. Oral Maxillofac. Surg.* **2001**, *59*, 185–190. [[CrossRef](#)] [[PubMed](#)]
131. Lanza, A.; Ruggiero, A.; Sbordone, L. Tribology and dentistry: A commentary. *Lubricants* **2019**, *7*, 52.
132. Lee, J.S.; Choi, H.I.; Lee, H.; Ahn, S.J.; Noh, G. Biomechanical effect of mandibular advancement device with different protrusion positions for treatment of obstructive sleep apnoea on tooth and facial bone: A finite element study. *J. Oral Rehabil.* **2018**, *45*, 948–958. [[CrossRef](#)]
133. Fernández-Rubio, E.M.; Radlanski, R.J. Development of the human primary and secondary jaw joints. *Ann. Anat.-Anat. Anz.* **2024**, *251*, 152169. [[CrossRef](#)] [[PubMed](#)]
134. Baragar, F.A.; Osborn, J.W. A model relating patterns of human jaw movement to biomechanical constraints. *J. Biomech.* **1984**, *17*, 757–767. [[CrossRef](#)]
135. Gregolin, R.F.; Zavaglia, C.A.d.C.; Tokimatsu, R.C.; Pereira, J.A. Biomechanical Stress and Strain Analysis of Mandibular Human Region from Computed Tomography to Custom Implant Development. *Adv. Mater. Sci. Eng.* **2017**, *2017*, 7525897. [[CrossRef](#)]
136. Koolstra, J.H. Biomechanical analysis of the influence of friction in jaw joint disorders. *Osteoarthr. Cartil.* **2012**, *20*, 43–48. [[CrossRef](#)] [[PubMed](#)]
137. Prado, F.B.; Rossi, A.C.; Freire, A.R.; Caria, P.H.F. The application of finite element analysis in the skull biomechanics and dentistry. *Indian J. Dent. Res.* **2014**, *25*, 390–397. [[CrossRef](#)] [[PubMed](#)]
138. Peck, C.C. Biomechanics of occlusion—Implications for oral rehabilitation. *J. Oral Rehabil.* **2016**, *43*, 205–214. [[CrossRef](#)] [[PubMed](#)]
139. Peck, C.C.; Hannam, A.G. Human jaw and muscle modelling. *Arch. Oral Biol.* **2007**, *52*, 300–304. [[CrossRef](#)] [[PubMed](#)]
140. Stavness, I.; Nazari, M.A.; Flynn, C.; Perrier, P.; Payan, Y.; Lloyd, J.E.; Fels, S. Coupled Biomechanical Modeling of the Face, Jaw, Skull, Tongue, and Hyoid Bone. In *3D Multiscale Physiological Human*; Springer: London, UK, 2013; pp. 253–274.
141. Eijden, T.M.G.J.; Korfage, J.A.M.; Brugman, P. Architecture of the human jaw-closing and jaw-opening muscles. *Anat. Rec.* **1997**, *248*, 464–474. [[CrossRef](#)]
142. Sagl, B.; Dickerson, C.R.; Stavness, I. Fast Forward-Dynamics Tracking Simulation: Application to Upper Limb and Shoulder Modeling. *IEEE Trans. Biomed. Eng.* **2019**, *66*, 335–342. [[CrossRef](#)] [[PubMed](#)]
143. Garcia, E.; Leal, M.M.; Villamil, M.B. Modeling and Simulation of Masticatory Muscles. *Procedia Comput. Sci.* **2015**, *51*, 2878–2882. [[CrossRef](#)]

144. Wang, X.; Xu, P.; Potgieter, J.; Diegel, O. Review of the biomechanics of TMJ. In Proceedings of the 19th International Conference on Mechatronics and Machine Vision in Practice (M2VIP), Auckland, New Zealand, 28–30 November 2012.
145. Daegling, D.J.; Hylander, W.L. Experimental observation, theoretical models, and biomechanical inference in the study of mandibular form. *Am. J. Biol. Anthropol.* **2000**, *112*, 541–551. [[CrossRef](#)]

Disclaimer/Publisher’s Note: The statements, opinions and data contained in all publications are solely those of the individual author(s) and contributor(s) and not of MDPI and/or the editor(s). MDPI and/or the editor(s) disclaim responsibility for any injury to people or property resulting from any ideas, methods, instructions or products referred to in the content.